Assimilation of Earth Rotation Parameters into a global ocean model: Length of Day excitation

Jan Saynisch[1], Manfred Wenzel[2] and Jens Schröter[2]

[1]: Helmholtz Centre Potsdam GFZ German Research Centre for Geosciences,

Earth System Modelling, Potsdam, Germany (saynisch@gfz-potsdam.de).

[2]: Alfred Wegener Institute for Polar and Marine Research, Climate Sciences - Ocean Dynamics,

Bremerhaven, Germany.

Okt. 2010

Abstract

Changes in the oceanic current system and in the oceanic mass distribution alter, together with other processes, the state of the Earth's rotation. This state is characterized by the length of day (LOD) and the tilt of the pole-to-pole axis. The aim of our study was to derive the respective governing physical mechanisms in the ocean. Therefore, Earth rotation observations were assimilated into a global circulation model of the ocean. Although assimilation is a well-established tool in climate science, the assimilation of Earth rotation observations into a global ocean model was done here for the first time. Prior to the assimilation, the Earth rotation observations were projected onto the angular momentum of the ocean. Non-oceanic contributions were removed. The result of the subsequent assimilation procedure is a time varying ocean model state that reproduces the projected Earth rotation observations well. This solution was studied to understand the oceanic generation of Earth rotation deviations and to identify governing physical mechanisms. This paper focuses on LOD anomalies although polar motion was assimilated simultaneously. Our results indicate that changes in the oceanic LOD excitation are mostly attributed to changes in total ocean mass. Changes in the spatial distribution of ocean mass turned out to have a minor contribution to the LOD deviations. The same applies to changes in the current system.

1 Introduction

The mean state of the Earth's rotation consists of one revolution per day around an axis which is tilted by about $23.5°$ compared with a vector normal to the ecliptic. Deviations from this mean state are described by the Earth rotation parameters (ERP). Deviations of the rotation period are called length of day (LOD) changes. Deviations in the tilt of the axis are called polar motion (PM). In the absence of external torques, these deviations are solely generated by terrestrial movements of mass. Mass movements may generate significant relative angular momentum or may change the Earth's tensor of inertia or both. The consequences are changes in the ERP. Therefore, the ERP observations contain superposed information about changes in Earth's mass movements and distribution. We aim to extract and separate this information via data assimilation.

The errors of ERP measurements are below one milliarcsecond for polar motion and a few microseconds for LOD anomalies (Gambis, 2004). In our study, we focus on information about the ocean, more precisely on the connection between LOD changes and oceanic processes.

The seasonal excitation of LOD change is dominated by the atmosphere (Rosen and Salstein, 1991). Longer time scales are dominated by very strong signals which are presumed to be caused by Earth's core and mantle (Gross et al., 2005; Pais and Hulot, 2000). Therefore, before assimilating ERP into an ocean model, the influences

of non-ocean Earth-systems have to be removed.

It is well known that assimilation of hydrological and oceanic data leads to better ERP estimates in models of land and ocean (Ponte et al., 2001; Chen, 2005). On the contrary, the assimilation of ERP observations itself, as presented here, is a very recent field of research. This approach can help to solve the problem that estimations of ocean angular momentum based on ocean circulation models are often much smaller than estimations based on observations (Ponte and Stammer, 2000; Chen, 2005).

The common approach to Earth rotation excitation follows Barnes et al. (1983):

$$\frac{\dot{m}_1}{\sigma_{ch}} + m_2 = \frac{\dot{\chi}_1}{\Omega} + \chi_2 \tag{1}$$

$$-\frac{\dot{m}_2}{\sigma_{ch}} + m_1 = -\frac{\dot{\chi}_2}{\Omega} + \chi_1 \tag{2}$$

$$\dot{m}_3 = -\dot{\chi}_3 \tag{3}$$

The m_i describe very small perturbations of the Earth's mean angular velocity vector and can be identified with polar motion (m_1, m_2) and length of day changes (m_3). The complex valued Chandler-frequency is symbolized by σ_{ch}. The absolute value of Earth's mean angular velocity is Ω.

The right-hand sides of (1)-(3) consist of the so called angular momentum functions χ_i. They force the deviations from the mean Earth rotation state. The angular momentum functions are called effective if they are written down in a form which accounts for loading and rotational deformation of the Earth's mantle (Barnes et al., 1983; Munk and MacDonald, 1960). Since this paper concentrates on LOD, only the axial effective angular momentum function is stated explicitly:

$$\chi_3 \equiv \frac{1}{C\Omega} \left(0.70\,\Omega\,\Delta\mathbb{J}_{33} + \Delta L_{r3} \right) \tag{4}$$

Here $\Delta\mathbb{J}_{33}$ describes small deviations in the respective component of Earth's tensor of inertia $\mathbb{J}$. The deviation in relative angular momentum ΔL_{r3} results from zonal mass movements relative to the rigid body rotation of the Earth, i.e., zonal ocean currents.

The remainder of this paper is structured as follows. The assimilation method is described in section 2. The used ocean model is characterized in section 3. The results of the OAM-assimilation experiments are presented

and discussed in section 4. We close with a summary in section 5.

2 Data assimilation method

An 4D-Var adjoint assimilation method is used to bring the angular momentum functions (χ_{mod}) of our ocean model closer to the corresponding observed values (χ_{obs}). The term "close" is thereby equivalent to the minimization of a quadratic, error ($\mathbf{W}$) weighted cost function (J):

$$J_\chi = (\chi_{mod} - \chi_{obs})^2 \mathbf{W}^{-1} \tag{5}$$

To minimize J the adjoint method alters a subset of the model parameters (Le Dimet and Talagrand, 1986). An adjoint version of our ocean model (see Sect. 3) calculates the gradient of the cost function J with respect to the models parameters. An iterative, quasi-Newtonian minimization algorithm was used to find a minimum of J (Gilbert and Lemaréchal, 1993). Despite the parameter change, the modeled physical laws remain unaffected by the minimization. Therefore, the result is a state estimate of the ocean which is entirely consistent with the model equations. Within this study the models control vector, i.e., parameters which are altered to minimize J, were the following: initial ocean state (i.e., velocities, temperatures, salinities and sea surface elevations) and the surface fluxes for every time step (i.e., heat, freshwater and momentum). The derivation of $\mathbf{W}$ is described in the following section. A more detailed description of the utilized assimilation procedure, the ocean model, the control parameters and the additional assimilation of oceanographic data can be found in Wenzel and Schröter (2007). We use here exactly the same approach as in Wenzel and Schröter (2007) with the only exception that we assimilate earth rotation parameters instead of sea level observations.

3 Model and data description

For the presented study we used a mass conserving version of the Large-Scale Geostrophic ocean model (LSG, Maier-Reimer et al., 1993). Following Greatbatch (1994) the mass conservation of this Boussinesq model is achieved by the modification of the sea level elevation. In contrast to Greatbatch (1994), who proposed a globally

uniform modification of the sea level, we used the local mass correction described in Wenzel and Schröter (2007).

The LSG is a 23-layer global circulation model with a horizontal resolution of 2.1°. Due to its implicit formulation this ocean model is stable even with a large time step of several days. The temporal resolution was chosen to be 10 days. In this configuration the ocean model is fast enough for the huge amount of iterations needed by the utilized assimilation procedure.

The LSG forcing consists of heat, freshwater and momentum fluxes which were derived from the respective datasets of NCEP/NCAR (Kistler et al., 2001). These datasets were decomposed into the leading 50 empirical orthogonal functions (EOF). Only the amplitudes of these EOF are allowed to change during the assimilation process. Due to the time step of 10 days the inverse barometer (IB) approximation can be used (Ponte, 2006). Therefore, no atmospheric pressure forcing is applied.

The assimilated effective ocean angular momentum functions (OAM) were derived as follows from the daily C04 ERP observations of the IERS (Gambis, 2004; Vondrak and Richter, 2004). The conversion of ERP measurements into angular momentum functions followed Gross (1992). The resulting three-component angular momentum functions describe the excitations from the whole Earth. Therefore, non-oceanic signals had to be removed before the assimilation. To this end, the IB atmospheric angular momentum functions (AAM) of the ECMWF's ERA-40 atmosphere reanalysis (Uppala et al., 2005) were calculated and subtracted (Dobslaw et al., 2010).

The reason for additionally including the freshwater-flux into the control vector is its large importance for ocean mass and the fact that it is poorly estimated by the atmospheric reanalyses (Trenberth and Smith, 2005; Hagemann et al., 2005).

The ERP were further corrected for the land hydrology. Here, the Hydrological Discharge Model (HDM) of Hagemann and Dümenil (1998) was utilized. The HDM model parameterizes surface flow, river flow and ground water. Runoff delays lead to variable water mass storage. The model contains an extended land-surface scheme which simulates soil moisture variations, evaporation and snow accumulation (Dill, 2008). This model realistically reproduces annual mean discharge (Dobslaw and Thomas, 2007) as well as the seasonal variations
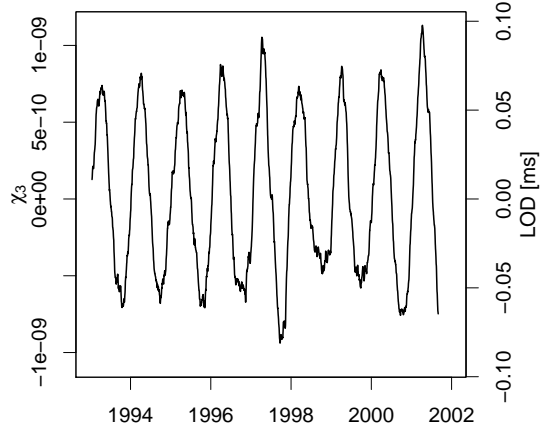

Figure 1: Axial effective angular momentum function of land hydrology model. The time series is highpass filtered.

of the land hydrology (see fig. 3). The axial effective HDM angular momentum is plotted in Fig. 1. The annual LOD amplitude is 0.1 ms and in good agreement with the CDAS-1 hydrological model of Chen et al. (2000) which also includes soil-moisture and snow accumulation. The polar motion excitation of the HDM model is also in good agreement with published results, e.g., Chen and Wilson (2005) (not shown, see Dobslaw et al., 2010).

The excitation of Earth rotation anomalies originating in the Earth's core and mantle was filtered out by a high-pass filter with a cut-off frequency of 1.5 years. The remaining residuum was resampled on the model time step and describes to a large extent the ocean angular momentum on monthly to annual time scales. To ensure consistency, the highpass filter was also implemented in the ocean models OAM observation operator. The same applies for the adjoint observation operator.

The biggest error in this projection comes from the uncertainty in the modeled atmospheric angular momentum (Masaki, 2008). A comparison of monthly AAM from ERA-40 with the respective NCEP/NCAR product reveals:

$$var(\chi_{NCEP} - \chi_{ERA40}) = \begin{pmatrix} 4.3 \times 10^{-16} \\ 4.6 \times 10^{-16} \\ 3.9 \times 10^{-19} \end{pmatrix} \quad (6)$$

The variances of uncertainties in the angular momentum functions derived from the ERP observations are comparatively small: $3.6 \times 10^{-19}, 3.5 \times 10^{-19}, 1.2 \times 10^{-19}$. The entries of (6) were used as weights $\boldsymbol{W}$ in equation (5). Since the contribution from land hydrology to the projection is very small the respective errors were neglected here. This is especially true for the LOD component where the atmosphere accounts for 80-90% of the observed variance (Hide and Dickey, 1991).

To ensure a reasonable model state as far as oceanographic features are concerned, additional oceanographic data were assimilated. These constraints consist of the following datasets: climatological profiles of salinity, temperature and velocity anomalies (Gouretski and Koltermann, 2004; Chapman, 1998); climatological means of the same quantities derived from the world ocean atlas (WOA, Conkright et al., 2002); monthly sea surface temperatures (Reynolds et al., 2002); quarterly temperatures of the upper ocean layers (0-750 m, Willis et al., 2004); mean internal transports of ocean mass and heat (Wijffels et al., 1992; Siedler et al., 2001). All datasets were interpolated onto the model time step of 10 days. For more details on these datasets please see Wenzel and Schröter (2007).

4 Results and discussion

As already mentioned the following analysis focuses on LOD. The ocean model state nonetheless was simultaneously fitted to the observations of PM, LOD and oceanographic measurements (see Sect. 3). To evaluate the enhancement due to the OAM-assimilation, we use a reference experiment that assimilates only the oceanographic datasets. The reference experiment and the OAM-assimilation experiment show realistic oceanographic behavior as was verified. e.g., by their meridional overturning circulations and their heat-content (not shown).

Figure 2 shows the effective axial ocean angular momentum function, i.e., the function which governs the LOD excitation. Compared to the reference experiment (red) the misfit between observation (black) and the model after OAM-assimilation (blue) is small. The reference experiment shares phase and frequency of the observation's annual cycle, but shows a too small variance on all frequencies. The OAM-assimilation experiment follows the
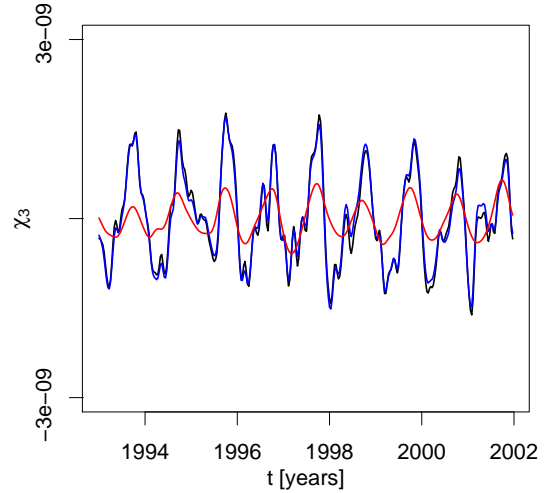

Figure 2: Ocean axial effective angular momentum function. Black: OAM Observations. Red: OAM of reference experiment. Blue: OAM of OAM-assimilation experiment. The time series are highpass filtered.

observations more closely. The rms of the misfit between model and observation reduces from 5.7×10^{-10} to 1.0×10^{-10}. This shows the potential of the presented assimilation procedure, but reveals also a limiting factor of the whole study. Compared to the square-root of equation (6), the achievable rms-values are already below the estimated uncertainty of the utilized AAM data. This means that the assimilated datasets do not contradict the modeled physics or each other. An overfitting of the ERP residuum does not raise the costs in other parts of the cost function (J). We conclude that given a more precise AAM time series the procedure would work equally well.

For the polar motion excitation the results are similar (not shown). The simultaneous reproduction of oceanographic data and all three ERP-components provides further evidence for the capabilities of the world oceans to generate sufficient angular momentum anomalies to explain the non-atmospheric ERP-residuals (e.g., Gross, 2000; Seitz et al., 2004). Further, our results are in agreement with the findings of Ponte et al. (2001) where assimilation of oceanographic data leads to better agreement with residual LOD observations. In detail, their approach reproduces the amplitude of the annual LOD cycle well. The
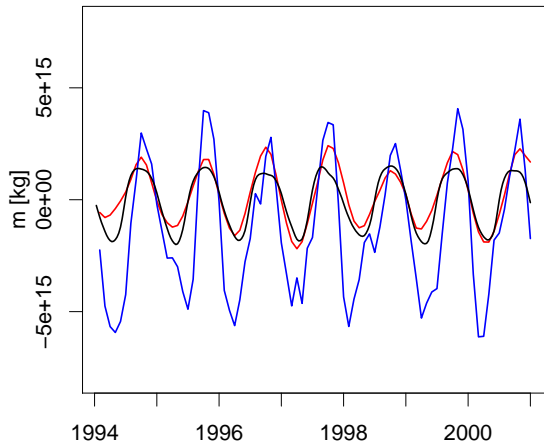
Figure 3: Total mass change due to freshwater-flux into the ocean. Black: hydrology model (only runoff). Red: Reference experiment. Blue: OAM-assimilation experiment. The time series are highpass filtered.
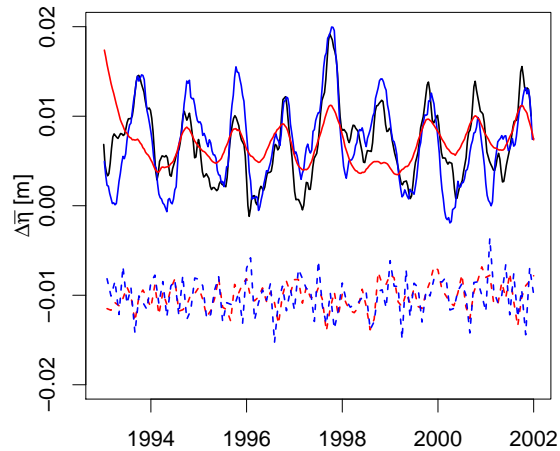

Figure 4: Global mean sea level (solid). Steric contributions (dashed). Black: Observations. Red: Reference experiment. Blue: OAM-assimilation experiment. For better distinction the global/steric values are moved up/down from the zero line. The time series are highpass filtered.

phases and the amplitudes of other frequencies are reproduced to a lesser extent. The additional assimilation of OAM observations, as shown here, reproduces the phase and amplitude of all assimilated frequencies.

The good reproduction of the LOD-observations in the assimilation-experiment is mostly due to an altered surface freshwater-flux compared to the reference experiment (Fig. 3). The annual freshwater cycle of the OAM-assimilation experiment was increased by the assimilation procedure to reproduce the higher annual LOD-variance. The total mass of the combined system of atmosphere, ocean and land hydrology should be conserved. To assess this point we included the land hydrology model, HDM, which we used for the reduction of ERP-observations into the comparison of the freshwater cycle.
The reference experiment (red) and the HDM (black) show a comparable annual cycle (rms = 0.6×10^{15} kg). The OAM-assimilation experiment (blue) has a significantly larger annual amplitude. These differences between land hydrology- and ocean model have to be evaluated with respect to the atmosphere. Estimates based on reanalyses-data of the mean annual change in global atmospheric water vapor range from 1.2×10^{15} kg to

1.5×10^{15} kg (Trenberth and Smith, 2005). The differences between the OAM-assimilation experiment and the HDM-runoff have a rms of 2.0×10^{15} kg and exceed the value of Trenberth and Smith (2005). Even more, not all of the 1.5×10^{15} kg are supposed to be stored in the ocean. But Trenberth and Smith (2005) argue also that the storage of water vapor in the atmosphere can be up to 0.5×10^{15} higher during ENSO events. In the end, these estimates are based on atmospheric reanalyses which showed serious problems in mass balance and freshwater flux (e.g., Hagemann and Gates, 2001; Trenberth et al., 2007).

To study this question further we compared our experiments with independent oceanographic observations. We will show that oceanic properties that are not assimilated profit from the OAM-assimilation as well. Furthermore, this will give arguments in favor of the altered freshwater-flux in the OAM-assimilation experiment. In Fig. 4 the global mean sea level from TOPEX/Poseidon and Jason satellite altimetry (T/P, Leuliette et al., 2004) is plotted. Again, the reference experiment (red) shares only phase and frequency of the annual cycle with the observations (black) but the variance is too small. Although the global

mean sea level was not assimilated the OAM-assimilation experiment (blue) fits the observations better. The rms of the misfit between model and observation reduces from 3.4 to 3 mm. Variance, phase and shape of the peaks are better reproduced. Even characteristic sea level deviations like the 1997/1998 El Niño are visible in the OAM-assimilation time series (see also Yan et al., 2002).

In our experiments, the steric contributions to the global mean sea level have a standard deviation of 1.6 mm in the reference experiment and 2.2 mm in the OAM-assimilation experiment. In contrast to the altimeter-based estimates from Willis et al. (2008) our steric sea level time series show a less clear annual signal and have smaller variance. As the temporal evolution of steric sea level contributions of the two experiments are very similar (dashed lines, Fig. 4) the better sea level agreement of the OAM-assimilation experiment has to be due to eustatic sea level change. This is in agreement with the higher freshwater-flux of the OAM-assimilation experiment which accounted also for the better LOD agreement (Fig. 3). This close connection of annual LOD and sea level is well known (Chen et al., 2000). While in Chen et al. (2000) an WOA-based estimate of the steric sea level was subtracted from the T/P-sea level observations our approach directly assimilates, among other temperature and salinity data, WOA-temperatures also. Not surprisingly, the results are comparable. However, as was discussed in Vinogradova et al. (2007) the relationship between OAM and sea level depends on the considered temporal and spatial scales. It becomes evident by comparing Fig. 4 with Fig. 2 that the assimilation of T/P-observations, as done in Ponte et al. (2001), enhances the modeled OAM even if OAM observations are not assimilated. The annual component will benefit most. Non-annual frequencies will not improve as much from the T/P-assimilation.

To understand in detail the generation of the oceanic LOD excitation in the OAM-assimilation experiment the summands of equation (4) are plotted separately (Fig. 5). The contribution from relative angular momentum (ΔL_{r3}, green) is small. The oceanic LOD excitation is dominated by changes in the tensor of inertia ($\Delta \mathbb{J}_{33}$, orange). Changes in the tensor of inertia can be caused by changes in ocean total mass and by changes in ocean mass distribution. To distinguish both, we plotted the OAM contribution from total ocean mass (dots in Fig. 5). The total ocean mass anomaly is a function of the boundary
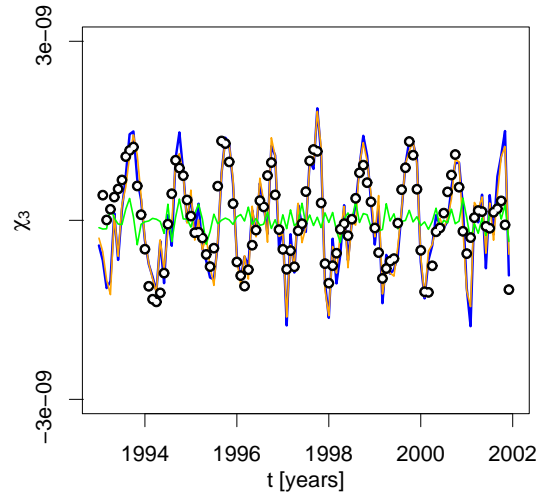

Figure 5: Axial OAM of the OAM-assimilation experiment split up into contributions from mass and currents, see equation (4). Orange: OAM anomalies due to tensor of inertia changes. Green: OAM anomalies due to changes of ocean currents. Dots: OAM anomalies due to total ocean mass change. The time series are highpass filtered.

freshwater-flux alone. Therefore, in the mass conserving LSG this contribution was computed by integrating the oceans surface freshwater-flux and assuming a globally uniform response in ocean bottom pressure. Since local pressure anomalies are globally equilibrated by, very fast, gravity waves this assumption is valid as far as our 10-day time step is concerned. On the considered monthly to annual time scales the changes in $\Delta\mathbb{J}_{33}$, that is the part of the tensor of inertia which contributes to the LOD excitation, result mostly from changes in total ocean mass (see also Fig. 3). The fraction of $\Delta\mathbb{J}_{33}$ which is not explained by total ocean mass change is small (misfit between dots and orange line) and must be attributed to spatial redistribution of ocean mass. This result seems to contradict Ponte and Stammer (2000), who use an ocean model with constant mass and still show a good coherence between ERP-residuals and OAM. But first, they state that their modeled OAM estimates are coherent, but substantially smaller than the residual ERP-observations and second, their ERP-reduction contains no land hydrology. Since ocean and land mass changes can cancel out (Chen et al., 2000) both statements could be true. A fraction of the small-amplitude ERP-AAM residuum can be explained with ocean mass redistribution while the large-amplitude ERP-(AAM+HAM) residuum can only be explained with global ocean mass change. We argue that for the reproduction of the right amplitude of oceanic LOD excitation an ocean model with free surface is necessary.

5   Summary

Effective angular momentum functions were calculated from ERP observations and were filtered for non-oceanic contributions. The residuum was assimilated into a global circulation model of the ocean. The successful reproduction of the three angular momentum components was done for the first time. In this paper, we show the implications for oceanic LOD excitation.

From the resulting ocean model trajectory the following conclusions could be drawn. Oceanic LOD excitation is to a large extent caused by changes in the oceanic tensor of inertia. These anomalies are generated via total ocean mass change. Changes in the ocean mass redistribution contribute only little to oceanic LOD excitation. The changes in the oceanic current system play also a mi-

nor role in oceanic LOD excitation. Further, it could be shown that the observed OAM can be used as proxy for the global mean sea level. At least on seasonal time scales the assimilation of the former determined the latter to a large extent. It turned out that the limiting factor for all this studies is the accuracy of the atmospheric excitation functions.

The ocean is also well able to excite substantial ERP signals on time scales both longer and shorter than considered here (Ponte and Ali, 2002; Landerer et al., 2007). Therefore, our next studies will utilize an ocean model with higher temporal resolution. We try to exchange the applied highpass filter with modeled data of Earth's core and mantle which became available only recently. Thus, it would be possible to study long-term variations of the global mean sea level also. We can summarize that the assimilation of Earth rotation observation has proved its potential and is currently only limited by the errors incorporated in the projection of Earth rotation observations onto ocean angular momentum.

References

Barnes, R. T. H., Hide, R., White, A. A., and Wilson, C. A. (1983). Atmospheric angular-momentum fluctuations, Length-Of-Day changes and Polar Motion. *Proc. R. Soc. London Ser. A-Math. Phys. Eng. Sci.*, 387(1792):31–73.

Chapman, P. (1998). The world ocean circulation experiment (WOCE). *Mar. Technol. Soc. J.*, 32(3):23–36.

Chen, J. L. (2005). Global mass balance and the length-of-day variation. *J. Geophys. Res.-Solid Earth*, 110(B8):B08404.

Chen, J. L. and Wilson, C. R. (2005). Hydrological excitations of polar motion, 1993-2002. *Geophys. J. Int.*, 160(3):833–839.

Chen, J. L., Wilson, C. R., Chao, B. F., Shum, C. K., and Tapley, B. D. (2000). Hydrological and oceanic excitations to polar motion and length-of-day variation. *Geophys. J. Int.*, 141(1):149–156.

Conkright, M. E., Locarnini, R. A., Garcia, H. E., O'Brien, T. D.and Boyer, T. P., Stephens, C., and Antonov, J. I. (2002). World ocean atlas 2001: Objective analysis, data statistics and figures. Technical report, National Oceanographic Data Center. CD-ROM Dokumentation.

Dill, R. (2008). Hydrological model LSDM for operational earth rotation and gravity field variations. Technical report, Helmholtz-Zentrum Potsdam Deutsches GeoForschungsZentrum.

Dobslaw, H., Dill, R., Groetzsch, A., Brzezinski, A., and Thomas, M. (2010). Seasonal polar motion excitation from numerical models of atmosphere, ocean, and continental hydrosphere. *J. Geophys. Res.*, 115:B10406.

Dobslaw, H. and Thomas, M. (2007). Impact of river runoff on global ocean mass redistribution. *Geophys. J. Int.*, 168(2):527–532.

Gambis, D. (2004). Monitoring Earth orientation using space-geodetic, techniques: state-of-the-art and prospective. *J. Geodesy*, 78(3-4):295–303.

Gilbert, J. C. and Lemaréchal, C. (1993). The modules M1QN3 and N1QN3. Version 2.0. Technical report, INRIA.

Gouretski, V. V. and Koltermann, K. P. (2004). WOCE global hydrographic climatology. Technical Report 35, Bundesamt für Seeschifffahrt und Hydrographie.

Greatbatch, R. J. (1994). A note on the representation of steric sea-level in models that conserve volume rather than mass. *J. Geophys. Res.-Oceans*, 99(C6):12767–12771.

Gross, R. S. (1992). Correspondence between theory and observations of polar motion. *Geophys. J. Int.*, 109(1):162–170.

Gross, R. S. (2000). The excitation of the Chandler wobble. *Geophys. Res. Lett.*, 27(15):2329–2332.

Gross, R. S., Fukumori, I., and Menemenlis, D. (2005). Atmospheric and oceanic excitation of decadal-scale Earth orientation variations. *J. Geophys. Res.-Solid Earth*, 110(B9):B09405.

Hagemann, S., Arpe, K., and Bengtsson, L. (2005). Validation of the hydrological cycle of era 40. Technical report.

Hagemann, S. and Dümenil, L. (1998). Documentation for the hydrological discharge model. Technical Report 17, Deutsches Klimarechenzentrum (DKRZ), Hamburg, Germany.

Hagemann, S. and Gates, L. D. (2001). Validation of the hydrological cycle of ECMWF and NCEP reanalyses using the MPI hydrological discharge model. *J. Geophys. Res.-Atmos.*, 106(D2):1503–1510.

Hide, R. and Dickey, J. O. (1991). Earths variable rotation. *Science*, 253(5020):629–637.

Kistler, R., Kalnay, E., Collins, W., Saha, S., White, G., Woollen, J., Chelliah, M., Ebisuzaki, W., Kanamitsu, M., Kousky, V., van den Dool, H., Jenne, R., and Fiorino, M. (2001). The NCEP/NCAR 50-year reanalysis. *Bull. Amer. Meteorol. Soc.*, 82(2):247–267.

Landerer, F. W., Jungclaus, J. H., and Marotzke, J. (2007). Ocean bottom pressure changes lead to a decreasing length-of-day in a warming climate. *Geophys. Res. Lett.*, 34(6):L06307.

Le Dimet, F. and Talagrand, O. (1986). Variational algorithms for analysis and assimilation of meteorological observations - theoretical aspects. *Tellus Ser. A-Dyn. Meteorol. Oceanol.*, 38(2):97–110.

Leuliette, E. W., Nerem, R. S., and Mitchum, G. T. (2004). Calibration of TOPEX/Poseidon and jason altimeter data to construct a continuous record of mean sea level change. *Mar. Geod.*, 27(1-2):79–94.

Maier-Reimer, E., Mikolajewicz, U., and Hasselmann, K. (1993). Mean circulation of the Hamburg LSG OGCM and its sensitivity to the thermohaline surface forcing. *J. Phys. Oceanogr.*, 23:731–757.

Masaki, Y. (2008). Wind field differences between three meteorological reanalysis data sets detected by evaluating atmospheric excitation of Earth rotation. *J. Geophys. Res.-Atmos.*, 113(D7):D07110.

Munk, W. H. and MacDonald, G. J. F. (1960). *The Rotation of the Earth: A geophysical discussion*. Cambridge University Press, Cambridge.

Pais, A. and Hulot, G. (2000). Length of day decade variations, torsional oscillations and inner core superrotation: evidence from recovered core surface zonal flows. *Phys. Earth Planet. Inter.*, 118(3-4):291–316.

Ponte, R. M. (2006). Oceanic response to surface loading effects neglected in volume-conserving models. *J. Phys. Oceanogr.*, 36(3):426–434.

Ponte, R. M. and Ali, A. H. (2002). Rapid ocean signals in polar motion and length of day. *Geophys. Res. Lett.*, 29(15).

Ponte, R. M. and Stammer, D. (2000). Global and regional axial ocean angular momentum signals and length-of-day variations (1985-1996). *J. Geophys. Res.-Oceans*, 105(C7):17161–17171.

Ponte, R. M., Stammer, D., and Wunsch, C. (2001). Improving ocean angular momentum estimates using a model constrained by data. *Geophys. Res. Lett.*, 28(9):1775–1778.

Reynolds, R. W., Rayner, N. A., Smith, T. M., Stokes, D. C., and Wang, W. Q. (2002). An improved in situ and satellite SST analysis for climate. *J. Clim.*, 15(13):1609–1625.

Rosen, R. D. and Salstein, D. A. (1991). A seasonal budget of the Earths axial angular-momentum - comment. *Geophys. Res. Lett.*, 18(10):1925–1926.

Seitz, F., Stuck, J., and Thomas, M. (2004). Consistent atmospheric and oceanic excitation of the Earth's free polar motion. *Geophys. J. Int.*, 157(1):25–35.

Siedler, G., Church, J., and Gould, J., editors (2001). *Ocean circulation and climate*.

Trenberth, K. E. and Smith, L. (2005). The mass of the atmosphere: A constraint on global analyses. *J. Clim.*, 18(6):864–875.

Trenberth, K. E., Smith, L., Qian, T., Dai, A., and Fasullo, J. (2007). Estimates of the global water budget and its annual cycle using observational and model data. *J. Hydrometeorol.*, 8(4):758–769.

Uppala, S. M., Kallberg, P. W., Simmons, A. J., Andrae, U., Bechtold, V. D., Fiorino, M., Gibson, J. K., Haseler, J., Hernandez, A., Kelly, G. A., Li, X., Onogi, K., Saarinen, S., Sokka, N., Allan, R. P., Andersson, E., Arpe, K., Balmaseda, M. A., Beljaars, A. C. M., Van De Berg, L., Bidlot, J., Bormann, N., Caires, S., Chevallier, F., Dethof, A., Dragosavac, M., Fisher, M., Fuentes, M., Hagemann, S., Holm, E., Hoskins, B. J., Isaksen, L., Janssen, P. A. E. M., Jenne, R., McNally, A. P., Mahfouf, J. F., Morcrette, J. J., Rayner, N. A., Saunders, R. W., Simon, P., Sterl, A., Trenberth, K. E., Untch, A., Vasiljevic, D., Viterbo, P., and Woollen, J. (2005). The ERA-40 re-analysis. *Q. J. R. Meteorol. Soc.*, 131(612, Part B):2961–3012.

Vinogradova, N. T., Ponte, R. M., and Stammer, D. (2007). Relation between sea level and bottom pressure and the vertical dependence of oceanic variability. *Geophys. Res. Lett.*, 34(3):L03608.

Vondrak, J. and Richter, B. (2004). International Earth Rotation and Reference Systems Service (IERS). *J. Geodesy*, 77(10-11):585–678.

Wenzel, M. and Schröter, J. (2007). The global ocean mass budget in 1993-2003 estimated from sea level change. *J. Phys. Oceanogr.*, 37(2):203–213.

Wijffels, S. E., Schmitt, R. W., Bryden, H. L., and Stigebrandt, A. (1992). Transport of fresh-water by the oceans. *J. Phys. Oceanogr.*, 22(2):155–162.

Willis, J. K., Chambers, D. P., and Nerem, R. S. (2008). Assessing the globally averaged sea level budget on seasonal to interannual timescales. *J. Geophys. Res.-Oceans*, 113(C6):C06015.

Willis, J. K., Roemmich, D., and Cornuelle, B. (2004). Interannual variability in upper ocean heat content, temperature, and thermosteric expansion on global scales. *J. Geophys. Res.-Oceans*, 109(C12):C12036.

Yan, X. H., Zhou, Y. H., Pan, J. Y., Zheng, D. W., Fang, M. Q., Liao, X. H., He, M. X., Liu, W. T., and Ding, X. L. (2002). Pacific warm pool excitation, Earth rotation and El Nino southern oscillations. *Geophys. Res. Lett.*, 29(21):2031.